




Cite this: *Sustainable Food Technol.*,  
2024, 2, 1757

# Modification of techno-functional and health-promoting properties of orange by-products through ultrasonication

Alina Manthei, Pedro Elez-Martínez, Olga Martín-Belloso and Robert Soliva-Fortuny \*

The orange juice extraction process generates significant amounts of by-products which currently lack practical applications leading to economic losses and potentially posing environmental threats. To enable their utilization, an orange pulp–peel powder mixture was subjected to different ultrasonication (US) input powers (200, 300, 400 W) and treatment times (15, 30, 45 min). Particle size was reduced with increasing treatment power and time which led to a maximum increase of 25.8% of water holding capacity (WHC), 12.9% of oil holding capacity (OHC) and 7.6% of bile acid adsorption capacity (BAC). Therefore, the highest treatment power and time (400 W, 45 min) were selected to be applied on mixtures comprised of different proportions of orange pulp and peel. PU80 contained 80% pulp and 20% peel, PU50 equal proportions and PU20 20% pulp and 80% peel. Solubility and content of crude fiber did not significantly change in the mixtures after US. However, WHC increased in all mixtures while OHC significantly improved in PU50 ( $8.16 \text{ g g}^{-1}$ ). Inhibition of  $\alpha$ -amylase (AAIR) and pancreatic lipase (PLIR) were enhanced in US treated PU80 and PU50. PU20 showed the highest increase of BAC from  $3.28 \text{ mg g}^{-1}$  to  $4.13 \text{ mg g}^{-1}$  after US which was related to an increase of the total phenolic content (TPC) in this treated mixture. This study could demonstrate that the efficacy of US in enhancing different properties of orange by-products highly depends on the ratio of orange pulp and peel in the by-product mixture, thus polysaccharide composition.

Received 16th July 2024  
Accepted 1st October 2024

DOI: 10.1039/d4fb00215f

[rsc.li/susfoodtech](https://rsc.li/susfoodtech)

## Sustainability spotlight

This study addresses the significant contribution of orange juice by-products to the global annual food waste. With approximately 25% of fruits and vegetables wasted post-harvest and during processing and the lack of application of the generated by-products, this research is crucial. We investigated the potential of ultrasonication treatments to improve the properties of orange by-product mixtures and achieved notable enhancements of certain dietary fiber properties, enabling future applications as a novel ingredient. This work aligns with the UN's Sustainable Development Goals, especially goal 12 for responsible consumption and production, by promoting sustainable practices and reducing waste. Transforming orange pulp–peel waste into valuable products not only mitigates environmental impact but also supports economic sustainability in the juice industry.

## 1 Introduction

Orange juice is one of the most preferred juices in the world generating high quantities of residues including the fruit peel and pulp, mainly flavedo (outer layer of orange peel), albedo (inner layer of peel) and segment walls.<sup>1</sup> A minor part of these residues is used for animal feed but most of the by-products are discarded, decompose in landfills and thereby contribute to greenhouse emissions.<sup>2</sup> Hence, it is urgent to prevent environmental problems caused by this side-stream. Since orange pulp and peel contain a high amount of dietary fiber (DF) and

bioactive components, they have high potential to be used as novel food ingredients to obtain high-DF food products.<sup>3,4</sup> The recommended intake of DF ranges from 18 to 38 g per day<sup>5</sup> and is associated with several beneficial effects on human health, such as a more diverse gut microbiota and attenuated blood glucose and cholesterol level leading to a lower risk for the development of coronary heart diseases, type 2 diabetes and obesity.<sup>6</sup> The pulp of an orange is constituted of about 55% total dietary fiber (TDF), therein 25% soluble dietary fiber (SDF),<sup>7</sup> whereas the peel contains mostly insoluble constituents, namely 48% insoluble dietary fiber (IDF) and 9% SDF.<sup>8</sup> Additionally, citrus peel has a higher content of polyphenolic and carotenoid substances than the pulp implying high antioxidant activity and antimicrobial effect.<sup>9,10</sup> However, the application of underutilized fractions from fruit and vegetables or their DF

Department of Food Technology, Engineering and Science, University of Lleida – Agrotecnio-CERCA Center, Av. Alcalde Rovira Roure, 191, 25198, Lleida, Spain.  
E-mail: [robert.soliva@udl.cat](mailto:robert.soliva@udl.cat)



extracts into food products often impairs the sensorial quality of the fiber-enriched end products, such as enhanced graininess, hardness and chewiness.<sup>11</sup> This is mainly due to the high IDF content of the by-products. Therefore, technological modification needs to be investigated to particularly decrease particle size and increase solubility towards a composition of 30–50% SDF content, which is associated with improved techno-functional, health-promoting and sensorial properties.<sup>12</sup> Changes of the molecular structure might be associated with higher antioxidant activity, hypocholesterolemic and -glycemic effect. Enhanced antioxidant properties are the result of the improved extractability of bioactive components, which were previously entrapped in the DF matrix.<sup>13,14</sup> Glucose and cholesterol reduction by DF are mainly based on the interaction of compounds, such as bile acids, cholesterol and digestive enzymes, with certain functional groups of the DF network and their physicochemical entrapment inside the DF network. This mechanism can be facilitated by a loosened DF network, higher SDF content and enhanced viscosity.<sup>15,16</sup> To achieve this objective, enzymatic and physical treatments, such as ultrasonication (US), high-pressure processing and extrusion, can be applied. US has shown high potential in enhancing the techno-functional and health-promoting properties of different DF sources, such as tea seed IDF,<sup>17</sup> garlic straw IDF<sup>18</sup> and cashew apple bagasse.<sup>19</sup> These enhancements primarily resulted from molecular alterations induced by high frequency US and acoustic cavitation. Applying US to a liquid medium generates fluid motion and microbubbles. These bubbles can grow when dissolved gas nuclei entries into a bubble or bubbles merge (coalescence).<sup>20,21</sup> When a certain size is reached, they collapse generating high shear forces, local increase of temperature and highly reactive radicals of the sonicated medium which can disrupt the molecular structure of polysaccharides.<sup>20,22</sup> To optimize the modification of DF properties, treatment conditions need to be selected carefully in terms of frequency, propagation of cycle (rest/work), energy applied and treatment time.<sup>23,24</sup> This work explored the impact of applying different US treatment conditions on the properties of an orange pulp–peel mixture. The aim was to identify conditions which enhance techno-functional and physiological DF properties. Applying a mixture ensures the utilization of both by-products and harnesses their distinct health benefits derived from their varying DF and polyphenolic compositions. Once selected the most appropriate US power and treatment time, the effect of the treatment on mixtures containing different proportions of pulp and peel was investigated, specifically focused on antioxidant, cholesterol- and glucose-reducing properties. This will provide a novel perspective on how modest changes in DF compositions impact the outcome of US application and property enhancement.

## 2 Methods

### 2.1 Preparation of orange pulp and peel powder mixtures

Oranges (*Navelina*), purchased from a local supermarket, were washed and the peel was removed and kept separately. The juice was extracted from the peeled fruit and the pulp was collected.

Peel and pulp were rinsed with distilled water at 85 °C and, after cooling down, with a solution containing 0.5% citric acid and 1% ascorbic acid to prevent the action of oxidizing enzymes.<sup>25</sup> Three washings with distilled water were added to reduce the glucose content to a minimum. Water was drained to the maximal extent and peel and pulp were dried in an oven at 55 °C for 72 h. The dried products were ground and sieved to a particle size of 0.5 mm. For treatments, orange pulp and peel powder were mixed in different proportions. Mixture PU80 was ascribed to the proportion of 80% pulp and 20% peel. Mixture PU50 contained equal quantities of pulp and peel and Mixture PU20 was composed of the highest proportion of peel (20% pulp/80% peel).

### 2.2 Ultrasonic treatment

US treatments were conducted with an US homogenizer (UP400S, Hielscher Ultrasonics GmbH, Teltow, Germany) with a frequency of 24 kHz and maximum input power of 400 W in continuous mode. Therefore, 4 g of pulp powder and 1 g of peel (mixture PU80) were mixed in 180 mL cold distilled water. This ratio was the maximum amount of substrate which could be added while still ensuring continuous mixing and minimal temperature increase during treatments. A sonotrode with a diameter of 14 mm and maximum amplitude of approx. 125 µm (H14, Hielscher Ultrasonics GmbH, Teltow, Germany) was immersed directly into the pulp–peel mixture suspension with a depth of 20 mm. To avoid thermal effects, the suspension was continuously cooled during treatments to maintain a temperature lower than 55 °C. Different input powers (50, 75, 100%, i.e. 200, 300, 400 W) and treatment times (15, 30, 45 min) were applied and the resulting products were labelled as 'T (for treated mixture) + power (in %) + time (in min)', i.e. 'T50-15' for a mixture treated with 50% power of the US device for 15 min, and 'T100-45' descriptive for a treatment applying 100% of power for 45 min, respectively (s. Table 1). The power intensities of T50, T75 and T100 were 36, 60 and 72 W cm<sup>-2</sup>, respectively. Following the determination of US power and time, treatments were carried out on PU50 (2.5 g pulp, 2.5 g peel) and PU20 mixtures (1 g pulp, 4 g peel) applying the previous described protocol and the selected conditions. For subsequent analysis, suspensions were frozen, lyophilized and the dried mixtures were ground and sieved to a particle size of 0.3 mm.

**Table 1** Summary of different US treatment conditions, applied to the pulp-rich mixture PU80 to find ideal conditions

|         | Input power [W] | Power intensity [W cm <sup>-2</sup> ] | Treatment time [min] |
|---------|-----------------|---------------------------------------|----------------------|
| T50-15  | 200             | 36                                    | 15                   |
| T50-30  | 200             | 36                                    | 30                   |
| T50-45  | 200             | 36                                    | 45                   |
| T75-15  | 300             | 60                                    | 15                   |
| T75-30  | 300             | 60                                    | 30                   |
| T75-45  | 300             | 60                                    | 45                   |
| T100-15 | 400             | 68                                    | 15                   |
| T100-30 | 400             | 68                                    | 30                   |
| T100-45 | 400             | 68                                    | 45                   |



### 2.3 Analysis of the DF properties of pulp-peel mixtures

The US treatment condition which induced the highest improvement of the properties of the PU80 mixture was selected based on measurements of particle size, water holding capacity (WHC), oil holding capacity (OHC) and bile acid adsorption capacity (BAC) of the differently treated mixtures (2.3.1 – 2.3.4). After selecting suitable conditions and applying them on PU50 and PU20 mixtures, determinations of particle size, WHC, OHC and BAC were carried out for mixtures PU50 and PU20 and additional analysis (2.3.5 – 2.3.10) was added for all untreated and treated mixtures.

**2.3.1 Particle size.** Particle size distribution was determined using a Malvern laser particle size analyzer (Mastersizer 3000, Malvern Instruments Ltd, Malvern, UK) with a wet dispersion unit (Hydro SM). The pulp-peel mixture suspension was measured before and after treatments in triplicate applying a particle refractive index of 1.333 with water as dispersant and aiming for a laser obscuration level between 70 and 80%. Analysis mode was set for non-spherical particles. ( $D_{50}$  and  $D_{[3,2]}$ ) of the particle size distribution were obtained from the device's software and used for further analysis.

**2.3.2 Water holding capacity.** For the determination of water holding capacity (WHC), 0.2 g of untreated and treated pulp-peel mixture was accurately weighed, mixed with 10 mL distilled water and let stand for 18 h.<sup>26</sup> Afterwards, the hydrated suspensions were filtered through a filter bag (FibreBags S, Gerhardt Analytical Systems, Königswinter, Germany). A portion of 10 mL distilled water was used to wash the centrifuge tube of insoluble remnants and additionally poured into the bag. The hydrated mass was left untouched until the excess of unbound water was drained, and the pellet was carefully weighed afterwards inside of the bag. WHC was calculated from the weight of the pulp-peel mixture ( $m_s$ ) and mass of the hydrated residue ( $m_h$ ) following eqn (1).

$$\text{WHC}[\text{g g}^{-1}] = (m_h - m_s)/m_s \quad (1)$$

**2.3.3 Oil holding capacity.** Following the method of Ma & Mu, (2016),<sup>27</sup> 0.2 g of pulp-peel mixture was weighed into a centrifuge tube, mixed with 20 mL sunflower oil and let stand for 2 h without stirring. The mixture was centrifuged at 2000 g for 20 min and the supernatant was carefully discarded. Oil holding capacity (OHC) was calculated from the weight of the pellet ( $m_p$ ) and the initial mass of the by-product mixture ( $m_s$ ) according to eqn (2).

$$\text{OHC}[\text{g g}^{-1}] = (m_p - m_s)/m_s \quad (2)$$

**2.3.4 Bile acid adsorption capacity.** Adsorption of bile acids capacity (BAC) was measured by mixing 0.2 g of pulp-peel mixture with 25 mL of 1 mg mL<sup>-1</sup> sodium cholate (Sigma-Aldrich, St. Louis, MO, USA) in 0.15 M NaCl solution at pH 7.<sup>28</sup> Samples were incubated at 37 °C for 2 h. Subsequently, the pulp-peel mixture suspension was centrifuged at 4000 g for 15 min and the supernatant was filtrated.<sup>29</sup> 200 µL of filtered

supernatant was added to 6 mL of 45% sulfuric acid, vortexed and after 5 min 1 mL 0.3% furfural was added. Samples were left to stand for 30 min at 60 °C in an incubator to induce the color reaction. After cooling down on ice, color was measured at 620 nm spectrophotometrically (UV-1600PC, VWR, PA, USA). The concentration of unbound sodium cholate was calculated by means of a cholate standard curve eqn (3).

$$\text{BAC}[\text{mg g}^{-1}] = (c_0 - c_s)/m_s \quad (3)$$

$c_s - c$  of unbound cholate in the supernatant  $c_0 - c$  of cholate in incubation solution  $m_s - m$  of pulp-peel mixture.

**2.3.5 Crude fiber and solubility.** The determination of crude fiber (CF), which quantifies the proportion of IDF components resistant to degradation by acid and basic solvents, followed the AOAC method 978.10 (1996). Therefore, 1 g of sample was weighed into a fiber bag (F57 fiber bags, ANKOM Technology, NY, USA), which was then carefully sealed by heat and placed in 250 mL beakers. Subsequently, petroleum ether was added until bags were fully covered. After 10 min, the solvent was removed, and bags were air dried. For extracting DF, bags were placed on trays of a fiber analyzer (Ankom Fiber analyzer, ANKOM Technology, NY, USA), 100 mL of 0.225 N H<sub>2</sub>SO<sub>4</sub> was added to the tray and extraction was conducted automatically by the device applying agitation and heat for 40 min. Afterwards, samples were washed with 1900 mL distilled water which was previously heated up to 75 °C to remove the acid residues. The three steps of extraction, *i.e.* washing with acid solution and twice with hot distilled water, were repeated by replacing the acid solution with 0.313 N NaOH. Subsequently, bags were removed from the device and excess water was carefully drained. Samples were placed in 250 mL beakers and covered with acetone for 5 min to remove fat from the mixtures. For drying, the bags containing the digested pulp-peel powders were placed on aluminum trays in the oven at 102 ± 2 °C until the dry matter reached constant weight. To determine ashes, bags with DF were incinerated at 600 ± 15 °C for 2 h and, after cooling down in a desiccator, weighed to assess the ash content and subtract it from CF.

For the measurements of solubility, 30 mL of distilled water was added to 0.2 g of pulp-peel powder mixtures and stirred for 3 h.<sup>30</sup> Samples were centrifuged at 3000 g for 20 min following by the filtration of the suspension through a filter paper (pore size: 13 µm; Dominique DUTSCHER SAS, Bernolsheim, France) applying vacuum to discard the supernatants. Residues were washed with 10 mL distilled water and dried at 60 °C for 24 h. Solubility was calculated applying eqn (4):

$$\text{Solubility}[\%] = ((m_s - m_{\text{dr}})/m_s) \times 100 \quad (4)$$

$m_{\text{dr}} - m$  of dried residue.

**2.3.6 Cholesterol adsorption capacity.** Cholesterol adsorption was measured using the method of Yang *et al.*, (2020)<sup>31</sup> with some modifications. Therefore, half of an egg yolk was diluted 1 : 10 with distilled water and homogenized with an Ultra Turrax (T 25 basic Ultra Turrax®, IKA Works GmbH & Co. KG, Staufen, Germany) at 13.500 rpm for 30 s to create a stable emulsion.



25 mL of this solution was mixed with 0.2 g of pulp-peel mixture and pH was adjusted to 7 to measure binding at intestinal conditions. Samples were incubated for 2 h at 25 °C since lower temperature needed to be applied to avoid flocculation of the egg yolk. Following centrifugation at 4000g for 15 min, supernatants were filtrated through filter bags. To measure the concentration of unbound cholesterol, 100 µL of the filtrate was mixed with 4 mL of acetic acid (90% v/v) and 0.1 mL of *o*-phthalaldehyde reagent composed of 50 mg of *o*-phthalaldehyde and 100 mL of glacial acetic acid. After 10 min, 2 mL of concentrated sulfuric acid was carefully added and samples were immediately vortexed. Absorbance was measured after 20 min incubation at 550 nm. The diluted egg yolk solution was used as a control. Cholesterol concentration was determined by utilizing a cholesterol standard curve of 0–2 mg mL<sup>-1</sup> cholesterol and calculated through eqn (5).

$$\text{CAC}[\text{mg g}^{-1}] = (c_0 - c_s)/m_s \quad (5)$$

$c_s$  –  $c$  of unbound cholesterol in the supernatant.  $c_0$  –  $c$  of egg yolk solution.

**2.3.7 Pancreatic lipase inhibition rate.** Pulp-peel mixture powder (0.1 g) was mixed with 10 mL sodium phosphate buffer (0.1 M, pH 7.2), 2 mL of olive oil and 1 mL of pancreatic lipase solution (0.75 mg in 1 mL buffer).<sup>32</sup> Samples were incubated for 1 h at 37 °C and enzyme reaction was inhibited by adding 15 mL of 95% EtOH. Centrifugation at 4000g for 15 min was conducted before titrating supernatants with 0.05 M NaOH by means of phenolphthalein as pH indicator. A control without by-product was carried along to calculate the inhibition of lipase activity (LIR) in producing free fatty acids by the pulp-peel mixtures (s. eqn (6)).

$$\text{LIR}[\%] = ((1 - V_s)/V_c) \times 100 \quad (6)$$

$V_s$  – titrated volume for sample.  $V_c$  – titrated volume for control.

**2.3.8  $\alpha$ -Amylase activity inhibition rate.** The inhibition rate of the activity of  $\alpha$ -amylase (AAIR) was determined following the method of Ma & Mu, (2016)<sup>27</sup> with slight modifications. Therefore, 0.5 g of the pulp-peel mixtures were mixed with 40 mL of a 4% (w/v) starch solution in 0.05 M phosphate buffer (pH 6.5) and 0.4%  $\alpha$ -amylase. Suspensions were filled into dialysis tubes with a molecular weight cut-off of 14 kDa (Sigma-Aldrich, St. Louis, MO, USA) and dialyzed against 200 mL of distilled water at 37 °C for 1 h. Controls of starch-amylase solutions without DF were carried along. After dialysis, the concentration of glucose in the dialysate was measured by means of a colorimetric assay using a glucose assay kit (Megazyme, Wicklow, Ireland). Therefore, 500 µL of sample was mixed with the GOPOD reagent, incubated for 20 min at 50 °C and absorbance at 510 nm was measured. The inhibition rate was calculated from the absorbance of the control  $A_c$  and of the sample  $A_s$  as shown in eqn (7).

$$\text{AAIR}[\%] = ((A_c - A_s)/A_c) \times 100 \quad (7)$$

**2.3.9 Antioxidant properties.** For the extraction of bioactive compounds, 0.8 g of pulp-peel mixture was added into 25 mL of 80% MeOH and mixed for 2 h (Chu *et al.*, 2019).<sup>29</sup> Afterwards, suspensions were centrifuged at 9000 rpm for 15 min, supernatants were filtered and used for further analysis.

**2.3.9.1 Total phenolic content.** Total phenolic content (TPC) was determined spectrophotometrically using microtiter plates. Therefore, 20 µL of extracts was mixed with 100 µL of 1 : 10 diluted Folin-Ciocalteu reagent and 75 µL of 7.5% Na<sub>2</sub>CO<sub>3</sub> was added.<sup>33</sup> Absorbance was measured at 765 nm after incubation of 1 h in the dark with a multiplate spectrophotometer (Multiskan™ GO, Thermo Fisher Scientific Inc., Waltham, MA, USA). A calibration curve with gallic acid from 0–100 µg mL<sup>-1</sup> aided the calculation of TPC in gallic acid equivalents (GAE) mg g<sup>-1</sup> following eqn (8):

$$\text{TPC}[\text{GAE mg g}^{-1}] = c(V/m_s) \quad (8)$$

$c$  – concentration of GAE from gallic acid standard curve [mg mL<sup>-1</sup>]  $V$  – volume of extract solution [mL]  $m_s$  –  $m$  of pulp-peel mixture used for extraction [g].

**2.3.9.2 Antioxidant activity – ABTS assay.** To assess the scavenging activity of antioxidants, a 7 mM ABTS<sup>•+</sup> stock solution and 140 mM potassium persulfate solution were prepared.<sup>34</sup> To produce ABTS<sup>•+</sup> radicals, potassium persulfate was added to the ABTS<sup>•+</sup> stock solution to a final concentration of 2.5 mM and the mixture was kept in dark for 16 h. Before measurements, ABTS<sup>•+</sup> radical solution was diluted with MeOH to an absorbance of  $0.70 \pm 0.05$  at 734 nm. The spectrophotometric assay was conducted by mixing 20 µL of extract solution with 220 µL of the diluted ABTS<sup>•+</sup> working solution following incubation of 6 min in dark.<sup>33</sup> Absorbance was measured at 734 nm and scavenging activity was expressed in Trolox equivalents (TE) [mg g<sup>-1</sup>] utilizing Trolox standards of 25–200 µM.

**2.3.10 ATR-FTIR.** The spectra of the untreated and treated orange pulp-peel mixtures were measured by a FT-IR spectrometer (FT/IR 6300, Jasco, Easton, MD, USA) from 650–4000 cm<sup>-1</sup> fitted with ATR device. The pulp-peel mixture powder was analyzed at a resolution of 4 cm<sup>-1</sup> and 2 mm s<sup>-1</sup> scanning speed for 2 : 30 min resulting in 128 scans.

## 2.4 Data analysis

Experiments were conducted twice for each treatment condition and, after selecting ideal treatment condition, three times for the different proportions of pulp-peel mixtures. Analysis of WHC, OHC and BAC was carried out in triplicate. Further experiments (2.3.5 – 2.3.10) were conducted in duplicate. The normality of the data was assessed using the Shapiro–Wilk test which indicated slight deviations from normal distribution. Additionally, a one-way ANOVA was performed on the results of each DF parameter. When statistical differences were found, a Tukey's HSD test ( $p < 0.05$ ) was conducted to compare groups.

## 3 Results and discussion

### 3.1 Impact of US treatment conditions

**3.1.1 Particle size.** US treatment decreased the average particle size ( $D_{50}$ ) and the surface mean ( $D[3,2]$ ) of the pulp-peel





**Table 2** Particle size ( $D_{50}$ ,  $D[3,2]$ ), water, oil holding and bile acid adsorption capacity (WHC/OHC/BAC) of untreated orange pulp–peel powder (NT) and after applying different US input powers (50, 75, 100%) and treatment times (15, 30, 45 min). Different letters indicate significant differences between samples ( $p < 0.05$ )

|         | $D_{50}$ [ $\mu\text{m}$ ] | $D[3,2]$              | WHC [ $\text{g g}^{-1}$ ] | OHC [ $\text{g g}^{-1}$ ] | BAC [ $\text{mg g}^{-1}$ ] |
|---------|----------------------------|-----------------------|---------------------------|---------------------------|----------------------------|
| NT      | $372.00 \pm 2.65^a$        | $90.17 \pm 1.63^a$    | $8.07 \pm 0.19^a$         | $6.35 \pm 0.13^{abc}$     | $3.70 \pm 0.04^{ab}$       |
| T50-15  | $314.00 \pm 7.00^b$        | $69.90 \pm 0.70^b$    | $9.13 \pm 0.15^b$         | $6.38 \pm 0.14^{abc}$     | $3.67 \pm 0.08^a$          |
| T50-30  | $306.33 \pm 7.09^b$        | $68.20 \pm 0.85^{bc}$ | $9.38 \pm 0.22^{bc}$      | $6.14 \pm 0.38^c$         | $3.62 \pm 0.13^a$          |
| T50-45  | $254.33 \pm 12.90^c$       | $67.03 \pm 0.15^c$    | $9.76 \pm 0.06^{cd}$      | $6.03 \pm 0.19^c$         | $3.64 \pm 0.02^a$          |
| T75-15  | $241.33 \pm 9.29^{cd}$     | $65.53 \pm 0.35^d$    | $9.78 \pm 0.18^{cd}$      | $6.29 \pm 0.19^{bc}$      | $3.74 \pm 0.08^{ab}$       |
| T75-30  | $220.67 \pm 5.86^d$        | $60.00 \pm 0.10^e$    | $9.87 \pm 0.03^d$         | $7.05 \pm 0.14^{ad}$      | $3.83 \pm 0.01^{abc}$      |
| T75-45  | $185.67 \pm 13.05^e$       | $59.90 \pm 0.61^e$    | $9.42 \pm 0.19^{bc}$      | $6.08 \pm 0.41^a$         | $3.82 \pm 0.09^{abc}$      |
| T100-15 | $198.00 \pm 4.36^e$        | $63.73 \pm 0.84^d$    | $9.86 \pm 0.08^d$         | $7.17 \pm 0.26^d$         | $3.91 \pm 0.03^{bc}$       |
| T100-30 | $137.67 \pm 2.08^f$        | $55.13 \pm 0.32^f$    | $10.10 \pm 0.08^d$        | $6.96 \pm 0.18^{abd}$     | $3.89 \pm 0.11^{bc}$       |
| T100-45 | $98.53 \pm 2.16^g$         | $45.13 \pm 0.65^g$    | $9.74 \pm 0.12^{cd}$      | $6.71 \pm 0.23^{abcd}$    | $3.98 \pm 0.06^c$          |

mixture suspension with increasing US treatment power and time (Table 2). The highest power (100%) and time (45 min) resulted in a decrease of 73.5% of  $D_{50}$  and 50% of  $D[3,2]$ . Hence, cavitation and the high shear forces during treatments caused the disruption of polysaccharide bonding resulting in a smaller particle size and the liberation and solubilisation of shortened polysaccharide fractions. Interestingly, the application of the longest treatment time in T50-45 and T75-45 achieved a similar decrease of  $D_{50}$  than shorter time but higher input power, *i.e.* T75-15 and T100-15. This emphasizes the impact of both parameters, US power and time, on the diminution of particle size and consequently the alteration of DF microstructure. Shown in Fig. 1, particle size distribution broadened when US was applied due to the gradual degradation of polysaccharides of a median particle size of 372  $\mu\text{m}$  (NT) to a size of 98.5  $\mu\text{m}$

(T100-45). Hence, US application primarily caused the fragmentation of larger particles into smaller fractions, leading to a wider range of particle sizes present in the treated mixtures and a general decrease in particle size across the distribution.

**3.1.2 Water and oil holding capacity.** Generally, the reduction of particle size and alteration of DF microstructure can lead to the enlargement of the surface area and exposure of hydrophilic and hydrophobic side chains and functional groups which improves water and oil binding.<sup>35,36</sup> WHC improved with all the selected treatment conditions (Table 2). The highest increase of 19.3% was observed for the by-product mixture treated with the highest power (T100) but without significant differences between treatment times, including T50-treated samples. Hence, no impact of US power and time could be observed. However, harsher treatment conditions, *i.e.* longer

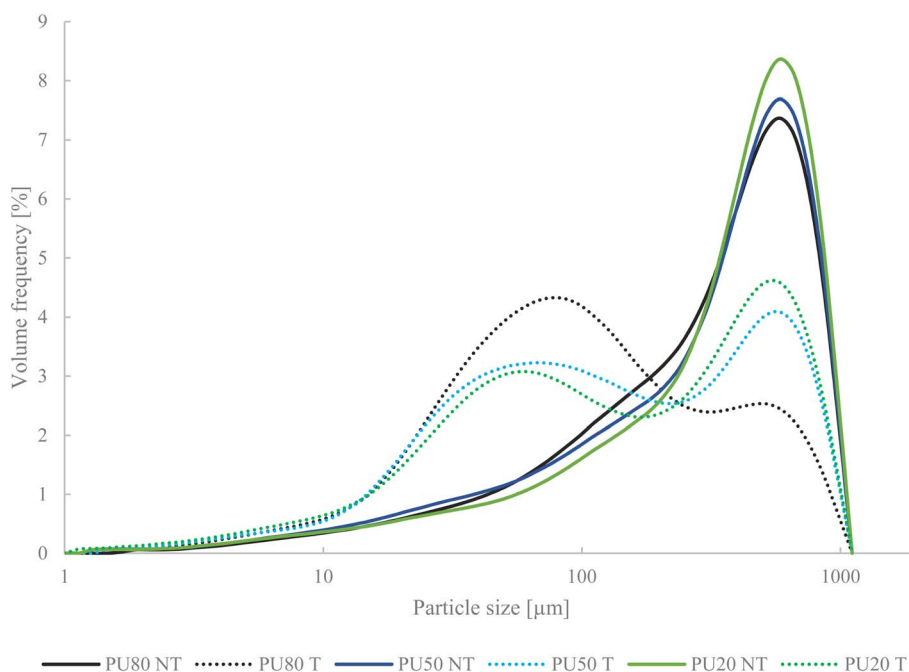


**Fig. 1** Particle size distribution of untreated (NT) pulp–peel mixtures and ultrasonically treated mixtures (T) with the selected treatment condition (T100 45). PU80 – 80% pulp, 20% peel, PU50 – 50% pulp, 50% peel, PU20 – 20% pulp, 80% peel.



treatment time and power, might favour higher improvements based on the lower particle size. Smaller particles imply an enlarged surface area which facilitate the interaction with water molecules.<sup>35</sup> Similarly, OHC was found to be highest in T100 samples with a maximum at T100-15 and an increase of 12.9% of this treatment condition to the untreated product. Other treatment conditions caused no significant changes. According to these results, US treatments could improve techno-functional properties of the orange pulp–peel mixture whereas maximal increases were achieved with the highest treatment power of 400 W. However, improvements were not affected by different treatment times since similar outcome could be achieved with only 50% of input power (200 W), particularly for WHC. Hence, the structural alterations, indicated by lower particle size, caused in T50-15 already might have been sufficient in opening the DF matrix and exposing mainly hydrophilic groups enhancing water-binding. On the contrary, results of OHC suggested that higher power was needed to cause structural modifications favourable to incorporate oil, thus there might be a progressive impact on surface hydrophobicity with higher power and treatment time. This is consistent with results from studies on the impact of different physical and enzymatic treatments on fruit or vegetable by-products. For instance, extrusion of orange pomace caused the increase of WHC but OHC and number of available hydrophobic, lipophilic groups decreased,<sup>37</sup> which was equally observed for the application of 600 MPa hydrostatic pressure treatments on carrot pomace IDF.<sup>38</sup> Hence, increase of WHC after structural modifications induced by the application of physical treatment seems to be more likely than OHC improvement.

**3.1.3 Bile acid adsorption capacity.** An important health-related property is the cholesterol-lowering effect of DF which is mainly based on the interaction with bile acids causing the delay of their diffusion and gastrointestinal adsorption and enhancing their excretion.<sup>15,39</sup> As a result, the catabolism of cholesterol to bile salts is promoted in order to maintain the bile salt pool.<sup>16</sup> Adsorption of these compounds requires direct molecular interaction with DF, thus being strongly based on DF composition and therein the availability of hydrophobic functional groups, mainly from polyphenols.<sup>15,40</sup> As shown in Table 2, BAC was gradually improved after US treatments with increasing power and time resulting in a significant improvement ( $p < 0.05$ ) in T100-45 ( $3.98 \text{ mg g}^{-1}$ ). BAC increase might be based on the progressive decrease of particle size, structural disruption and partial solubilization by US which opened DF structure and enhanced the accessibility of certain functional groups. A study with different soluble and insoluble DF sources showed that a higher SDF content contributed to a higher BAC since apple SDF demonstrated higher BAC than insoluble soybean hull and wheat bran IDF as well as its addition to a mixture of these IDF sources.<sup>41</sup> Oil binding and BAC often correlate since both are dependent on the availability of hydrophobic groups.<sup>29,42</sup> The similar tendency of applying higher power and achieving higher OHC and BAC could be observed but OHC did not show the same gradual increase than BAC and its maximum was reached at T100-15. Since bile acids can not only be retained by hydrophobic interactions, but also

by electrostatic interactions, more factors, such as ionic strength, play a role in their adsorption.<sup>16,43</sup> Additionally, high structural alterations and particle size reduction, as in T100-45, is likely to cause a partial structural damage of the DF framework which highly affects oil binding. In line with these observations, extruded orange pomace DF exhibited an increase of BAC but decrease of OHC.<sup>44</sup> As US was conducted in water, it may not enhance the structural properties that favor oil retention but rather increase the surface area available for water binding, thus also improving BAC which was measured in a water-based medium. This might have led to the absent correlation between particle size, OHC and BAC.

### 3.2 Relevance of orange pulp and peel proportions for the enhancement of DF properties by US

Low particle size of a fiber-rich ingredient is an important factor for its potential application since smaller particles are attributed with higher solubility and thereby improved product stability, such as enhanced emulsion stability, moisture retention and shelf-life,<sup>45</sup> and minimized impact on the alteration of sensory properties, *e.g.* graininess and crispiness.<sup>46</sup> Therefore, T100-45, *e.g.* 400 W for 45 min, was chosen as most favorable condition for further analysis. Additionally, T100-45 showed enhanced WHC and BAC which ascribed higher thickening and health-promoting properties to this ingredient.

**3.2.1 Physicochemical properties: particle size, crude fiber and solubility.** As shown in Table 3, the application of US resulted in the decrease of  $D_{50}$  of PU50 and PU20, corresponding to the findings in treated PU80 (s. 3.1.1). Orange peel showed a higher particle size than the pulp indicated by the higher  $D_{50}$  of PU20 ( $424.33 \mu\text{m}$ ). After applying the selected US treatment (T100 45), lower reduction of the particle size was achieved in PU50 and PU20 (PU50: 66%, PU20: 64.4%) compared with the decrease in PU80 (73.5%). This demonstrated a higher resistance of the particles of orange peel to US degradation which might be the result of a more rigid plant cell wall structure of the peel based on a higher cellulose content and tight entanglement of the cellulose and lignin networks.<sup>47</sup> To evaluate the impact on the DF composition, solubility and the content of crude fiber (CF), which includes mainly IDF fractions of cellulose, hemicellulose and lignin which were not degradable by acid and basic solvents, were measured. Solubility provides an approximate value of the SDF content in the DF material with a slight overestimation as other soluble components of the complex matrix are considered resulting in higher values than the actual SDF content.<sup>48</sup> PU80 contained more CF (NT: 21.87%) than PU20 (NT: 15.53%) which implied a higher CF content to orange pulp compared to the peel (Table 3). US applications did not affect CF in PU80 but led to a moderate decrease of insoluble CF components in PU50 and PU20 without statistical significance. Solubility of the mixtures ranged from 41.40% (untreated PU80) to 45.57% (treated PU20). Although there was no significant effect of US on the solubilities of the pulp–peel mixtures, the percentage of soluble components tended to increase which might indicate moderate depolymerization by US. Increases were slightly higher in PU50



**Table 3** Physicochemical characteristics, including  $D_{50}$  of particle size distribution, CF content and solubility, and cholesterol-reducing properties, i.e. bile acid and cholesterol adsorption capacity (BAC/CAC), of untreated (NT) and treated (T) pulp–peel mixtures. PU80 – 80% pulp, 20% peel, PU50 – 50% pulp, 50% peel, PU20 – 20% pulp, 80% peel<sup>a</sup>

|         | $D_{50}$ [ $\mu\text{m}$ ] | CF [%]                | Solubility [%]        | BAC [ $\text{mg g}^{-1}$ ] | CAC [ $\text{mg g}^{-1}$ ] |
|---------|----------------------------|-----------------------|-----------------------|----------------------------|----------------------------|
| PU80 NT | $372.0 \pm 2.65^a$         | $21.87 \pm 1.12^a$    | $41.40 \pm 0.27^a$    | $3.70 \pm 0.04^a$          | $5.34 \pm 0.48^a$          |
| PU80 T  | $98.53 \pm 25.0^b$         | $21.98 \pm 1.27^a$    | $42.46 \pm 0.43^{ab}$ | $3.98 \pm 0.06^{ab}$       | $4.88 \pm 0.30^{ab}$       |
| PU50 NT | $387.67 \pm 4.16^c$        | $19.59 \pm 0.08^{ab}$ | $41.86 \pm 0.36^{ab}$ | $3.95 \pm 0.05^{ab}$       | $4.73 \pm 0.37^{ab}$       |
| PU50 T  | $131.67 \pm 4.62^d$        | $17.81 \pm 0.58^{bc}$ | $43.24 \pm 0.20^{ab}$ | $3.83 \pm 0.10^a$          | $3.14 \pm 0.07^b$          |
| PU20 NT | $424.33 \pm 2.89^e$        | $15.53 \pm 0.60^{cd}$ | $42.19 \pm 0.38^{ab}$ | $3.28 \pm 0.22^c$          | $3.33 \pm 0.73^b$          |
| PU20 T  | $151.33 \pm 3.06^f$        | $14.47 \pm 0.75^d$    | $45.57 \pm 1.15^b$    | $4.13 \pm 0.15^b$          | $3.02 \pm 0.69^b$          |

<sup>a</sup> CF – crude fiber, BAC – bile acid adsorption capacity, CAC – cholesterol adsorption capacity.

and PU20, aligning with the decrease of CF in these samples. Results are in accordance with the study of Tejada-Ortigoza *et al.*, (2018)<sup>49</sup> who reported solubilities of 34.0–36.6% of orange peel residues with no significant increase after applying high hydrostatic pressure and mild heat treatments. In line with the observed CF decreases alongside increased solubilities, Garcia-Amezquita *et al.*, (2018)<sup>30</sup> determined solubilities of orange peel and prickly pear concentrates ranging from 34.4% to 53.9% showing a negative correlation with their IDF contents.

To summarize, the application of US possibly caused a moderate increase of solubilized DF components in the mixtures with higher peel concentrations, but overall, US treatments demonstrated limited efficacy in solubilizing orange pulp/peel IDF. Higher US input power than 400 W might be required to achieve more severe disruption of the IDF matrix.

**3.2.2 Techno-functional properties: water and oil holding capacity.** The impact of US cavitation on techno-functional properties is illustrated in Fig. 2. WHC improved significantly in PU80 and PU50 ( $p < 0.05$ ) but not in PU20 after applying US cavitation. PU80 exhibited the highest WHC before ( $8.07 \text{ g g}^{-1}$ ) and after modification ( $9.74 \text{ g g}^{-1}$ ) while the higher content of

orange peel conferred lower WHC to mixtures PU50 and PU20. Oil binding properties did not significantly change in PU80 and PU20. However, PU50 containing equal proportions of pulp and peel exhibited an increase of 29% to  $8.16 \text{ g g}^{-1}$  after US. As already discussed in 3.1, the basis of high WHC is the availability of hydrophilic groups and the capacity to build mesh structures incorporating water inside of the DF network.<sup>36</sup> Consequently, the increased quantity of orange pulp in PU80 possibly implied a higher number of water-binding sites, such as hydroxyl and carboxyl groups, to this mixture. Additionally, its higher CF content but lower particle size must have facilitated the formation of a network-like IDF matrix structure enabling the incorporation of greater amounts of water and conferring a thickening effect to this ingredient. After US application, the availability of hydrophilic groups in pulp-rich mixtures PU80 and PU50 must have been enhanced due to a loosening effect of the physical treatment on DF structures. As observed for the applications of different treatment conditions in 3.1, the higher decrease of particle size in PU80 was positively linked with the higher WHC enhancement and confirmed the importance of particle size reduction for water binding properties. The exclusive enhancement of OHC in PU50 underlined the high dependence of treatment effectiveness on the ratio of pulp and peel within the mixture, thereby highlighting the importance of DF molecular structure, polysaccharide composition and initial availability of functional groups. The increased OHC after US of PU50 might be the result of the interaction of lipophilic sites of pulp and peel components or/and increased charge density in this mixture.<sup>42</sup> In accordance with these results, US treatments with similar treatment conditions on garlic straw IDF induced an increase of WHC, from  $7.38 \text{ g g}^{-1}$  to  $9.72 \text{ g g}^{-1}$ , related to a more porous structure and correspondingly a higher surface area.<sup>18</sup> Extrusion of orange pomace led to a comparable increase of 16.0% in WHC but decrease of OHC.<sup>50</sup>

**3.2.3 Antioxidant properties.** Results of total phenolic content (TPC) and antioxidant activity, measured by ABTS<sup>+</sup> scavenging, are shown in Fig. 3. Mixture PU80, containing the highest proportion of orange pulp, exhibited the lowest TPC and antioxidant activity (NT:  $11.06 \text{ GAE mg g}^{-1}$ ,  $3.55 \text{ TE mg g}^{-1}$ ). The increase of the amount of orange peel in PU50 and PU20 corresponded to the enhancement of TPC and ABTS<sup>+</sup> scavenging rates. In line with that, Athanasiadis *et al.*, (2022)<sup>51</sup>

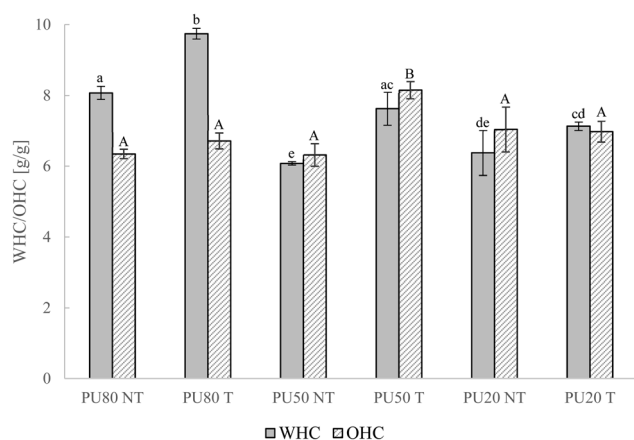


**Fig. 2** Water and oil holding capacities (WHC/OHC) of not-treated (NT) pulp–peel mixtures and ultrasonically treated (T) mixtures with the selected treatment condition (T100 45). Mix PU80 – 80% pulp, 20% peel, PU80 – 80% pulp, 20% peel, PU50 – 50% pulp, 50% peel, PU20 – 20% pulp, 80% peel. Different letters indicate significant differences between samples ( $p < 0.05$ ); lowercase: differences in WHC, capitalized: differences in OHC.



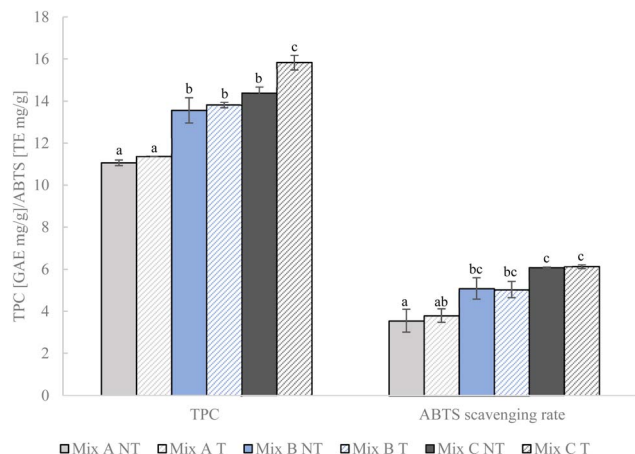


Fig. 3 Total phenolic contents (TPC) and ABTS scavenging rates of not-treated (NT) pulp–peel mixtures and ultrasonically treated (T) mixtures with the selected treatment condition (T100 45). PU80 – 80% pulp, 20% peel, PU50 – 50% pulp, 50% peel, PU20 – 20% pulp, 80% peel.

compared the composition of antioxidants of orange pulp (albedo) and peel (flavedo) and attributed a significantly higher content of ascorbic acid, carotenoids and polyphenols to orange peel. The same study identified hesperidin and chlorogenic acid as the predominant polyphenols in orange peel which might be the primary contributors to the enhanced TPC in PU20. Considering that hesperidin is associated with several health-promoting effects, such as anti-inflammatory and antimicrobial properties,<sup>52</sup> this imparts a significant health-promoting potential to orange peel.

After applying US, there were no significant changes of TPC observed in the extracts derived from mixtures PU80 and PU50 containing higher concentrations of orange pulp (Fig. 3). However, TPC significantly increased from 14.39 GAE mg g<sup>-1</sup> to 15.83 mg g<sup>-1</sup> in PU20 ( $p < 0.05$ ). Hence, US could enhance the extractability of polyphenolic compounds in orange peel which were previously bound to polysaccharides and entrapped in the DF matrix. On the contrary, it might suggest a higher availability of polyphenols and a lower amount of non-extractable polyphenols in orange pulp. Nevertheless, as shown in Fig. 3, ABTS<sup>•+</sup> scavenging rates were not impacted by US in all mixtures. In many studies, the enhancement of TPC by physical modification, such as high-pressure treatment of citrus peel<sup>9</sup> and ball milling combined with high-pressure of citrus fiber<sup>53</sup> correlated with the improvement of radical scavenging. Discrepancies could be due to a reduced activity of polyphenols caused by high temperatures during treatments, a decrease of the concentration of other bioactive compounds, such as ascorbic acid and carotenoids, or/and a shift of the concentrations of different polyphenolic components possessing different antioxidant activities.<sup>9</sup> Since the Folin–Ciocalteu reagent lacks specificity and can react with other reducing substances, such as ascorbic acid and sugars, or exhibit varying responses to different polyphenolics based on their structure, a higher TPC value does not necessarily indicate a higher antioxidant capacity. Furthermore,

Lohani *et al.*, (2016)<sup>54</sup> found that increasing temperatures during US cavitation of apple pomace negatively impacted the content of extracted polyphenolic compounds and their antioxidant activity, with a decrease evident above 45 °C. Additionally, lower levels of ascorbic acid and carotenoids after US should be considered in the assessment of ABTS<sup>•+</sup> scavenging of PU20. It was reported that the instability of ascorbic acid increased with temperatures above 40 °C.<sup>55</sup> A study carried out by Murador *et al.*, (2019)<sup>56</sup> observed the temperature-dependent degradation of xanthophylls, the main carotenoids found in orange peel by-products. Although cooling was applied during treatments, high local temperature increase cannot be avoided particularly when US is conducted in continuous mode. However, it is important to note that there are also studies indicating the opposite outcome of an enhancing effect on the solubility of polyphenolic compounds by mild heat treatments around 70 °C which indicates varying temperature sensitivities among carotenoids and polyphenols.<sup>57,58</sup> These factors might have contributed to the varying impact of US in the mixtures with distinct antioxidant profiles.

**3.2.4 Cholesterol-reducing properties: bile acid and cholesterol adsorption capacity, pancreatic lipase inhibition rate.** Cholesterol reduction of the pulp–peel mixtures was assessed by measuring BAC, adsorption capacity of cholesterol (CAC) and pancreatic lipase inhibition rate (PLIR). The impact of US on BAC in the pulp–peel mixtures varied (Table 3). As discussed in 3.1.3, moderate increase in PU80 was achieved with the selected conditions of US. However, US did not affect BAC in PU50 but induced an increase of 25.8% in PU20 to 4.13 mg g<sup>-1</sup>. This improvement must have been the result of enhanced TPC in the treated pulp–peel mixture which is in accordance with the results of Naumann *et al.*, (2020)<sup>59</sup> and Hamazu & Suwannachot, (2019)<sup>40</sup> who proposed a link between BAC and polyphenols. However, results revealed that the content of polyphenolics did not play the key role in BAC since the untreated peel-rich mixture PU20 showed the lowest BAC (3.28 mg g<sup>-1</sup>) among the mixtures but had significantly higher TPC than PU80. Of higher importance might be the type of polyphenolic component and its accessibility within the DF structure. According to the polyphenolic profile of orange pulp and peel, the flavanone nairutin is the only component which was found in much higher concentration in orange pulp.<sup>51</sup> Hence, nairutin might be a component contributing to high BAC. Another influencing factor for the enhancement of BAC in PU20 might have been the release of lipophilic components present in orange peel, particularly limonene and carotenoids.<sup>60</sup> On the other hand, the higher amount of orange pulp might have favored ionic interactions and have contributed to the higher BAC in untreated PU80 and PU50. Pectin, as a charged and polarizable molecule, can support electrostatic interactions.<sup>61</sup> Hence, higher pectin availability, enhanced surface area,<sup>62</sup> promoted by the lower particle size, and less entanglement of lignin and cellulose<sup>63</sup> in the orange pulp of PU80 and PU50, could be additional factors leading to the enhanced BAC of untreated mixtures containing higher orange pulp concentrations.





As presented in Table 3, US treatment had no significant effect on CAC of orange pulp–peel mixtures although a slight reduction after US particularly in PU50 could be observed. However, orange pulp exhibited higher adsorptive properties than the peel since CAC decreased in the following order: PU80 ( $5.34 \text{ mg g}^{-1}$ ) > PU50 ( $4.73 \text{ mg g}^{-1}$ ) > PU20 ( $3.33 \text{ mg g}^{-1}$ ). The lower CAC of orange peel might approve the impeded accessibility of certain functional groups in the substrate which was indicated by the low BAC of untreated PU20. Benitez *et al.*, (2019)<sup>32</sup> suggested that CAC is mainly related to chemical groups of the hemicellulose and cellulose fraction of IDF. This was confirmed since the slight decrease of CAC after US in all mixtures and particularly the low CAC of PU20 must correspond with the reduced content of CF in these samples. Similarly, enzymatically treated tea seed fiber did not show any improvement of CAC<sup>17</sup> as well as fermentation and microwave treatment of okara DF.<sup>64</sup> However, extrusion of orange pomace DF<sup>37</sup> or high-pressure processing of pear pomace<sup>65</sup> resulted in CAC enhancements although IDF contents were reduced. The binding mechanism of cholesterol to DF structures is still not clear but SDF components might play an important role.<sup>66</sup> However, centrifugation methods evaluate primarily binding of IDF but are not suitable to measure adsorptive properties of SDF. Our results indicate that US cavitation of the orange by-product mixtures caused structural and functional changes in IDF which impaired cholesterol adsorption.

PLIR of DF is an additional factor which highly impacts blood cholesterol and triglyceride level. Since lipase hydrolyzes triglycerides to glycerol and fatty acids, the inhibition of its activity delays fat absorption and reduces circulating triglycerides and cholesterol.<sup>67</sup> As shown in Fig. 4, US treatment led to a 1.9fold increase of PLIR in PU80 to 17.65% and 3.1fold enhancement in PU50 to 18.91%. Mixture PU20 showed the highest PLIR among the untreated by-product mixtures (12.18%) but was not affected by US modification. The higher

PLIR in PU20 when comparing the untreated samples must be associated with its higher orange peel and TPC content. R. Huang *et al.*, (2020)<sup>68</sup> compared the PLIR of different citrus peel extracts and could assign significant inhibition capacity to hesperidin which is abundant in orange peel. However, improvements after US in orange pulp-rich mixtures PU80 and PU50 must correlate with different structural characteristics, mainly solubility and pectin increase. Pectin polysaccharides can stimulate bridging flocculation of lipids by binding to lipid droplets which leads to decreased interfacial surface area and impeded access of triacylglycerides for lipase and thereby reduced lipolysis.<sup>69</sup> Flocculation and inhibition are dependent on the concentration and structure of pectin polysaccharides.<sup>70</sup> Therefore, the release or facilitated accessibility of some pectin poly- or oligosaccharides of orange pulp in PU80 and PU50, indicated by lower particle size and enhanced solubility, might have favored lipid droplet aggregation and inhibited lipase activity.

**3.2.5  $\alpha$ -Amylase inhibition rate.** The inhibition of  $\alpha$ -amylase by DF has a high impact on blood glucose reduction since impeded activity of the enzyme lowers starch degradation to glucose. Results of  $\alpha$ -amylase inhibition rates (AAIR) are presented in Fig. 4 showing highest AAIR (NT: 26.13%, T: 33.88%) in PU80, which is rich in orange pulp. Similar to lipase inhibition, US achieved high improvements of AAIR in PU80 and PU50 (29.8% increase in PU80 and 54.7% in PU50) but a 20.0% decrease in PU20. These results suggest a higher hypocholesterolemic and -glycemic effect for the ultrasonicated mixtures with a higher content of orange pulp. According to different study results, the main mechanism of AAIR by DF is the entrapment of enzyme and starch inside the DF matrix and/or their adsorption by DF components leading to a reduced accessibility of starch to the enzyme and decelerated hydrolysis.<sup>71</sup> Ma & Mu, (2016)<sup>27</sup> highlighted the role of high SDF and viscosity in enhancing AAIR since these factors support the capture mechanism and reduced contact rate of amylase and its substrate. Based on these findings, the increase in PU80 and PU50 after US could be associated with the elevated WHC in these samples. In addition, higher CF contents in these products might have contributed to direct adsorption since cellulose was reported to be highly effective in binding  $\alpha$ -amylase.<sup>71</sup> Since a similar trend, *i.e.* increasing impact in PU80 and PU50 but adverse effect in the orange peel-dominant mixture PU20, was observed for PLIR and this was likely linked to pectin concentrations, the inhibiting effect of pectin on  $\alpha$ -amylase activity must be considered as a contributing factor. Bai *et al.*, (2021)<sup>72</sup> confirmed the inhibition of the enzyme by purified pectin and pectin oligosaccharides and emphasized the importance of the structural characteristics of pectin, such as the degree of methyl-esterification, for AAIR.

**3.2.6 Effect on chemical structure – ATR-FTIR.** Structural differences regarding the functional groups of DF were analyzed by ATR-FTIR. Untreated and treated orange pulp–peel mixtures had similar spectral profiles but mixtures after US showed weakened intensities at some bands indicating the detachment of the associated DF components by the physical treatment (Fig. 5). Treated PU50 showed the highest deviations from its

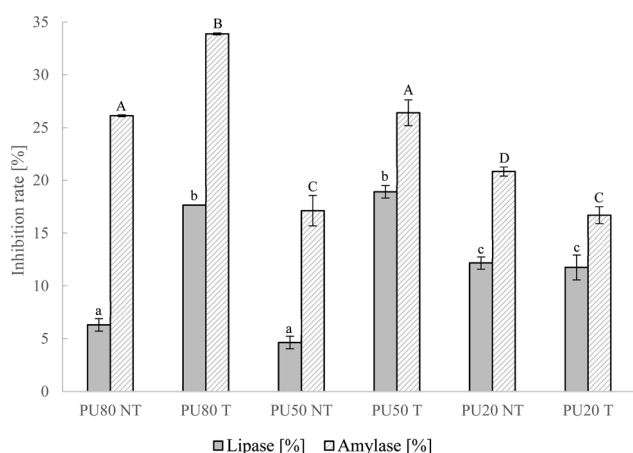
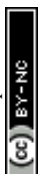


Fig. 4 Inhibition rates of pancreatic lipase and  $\alpha$ -amylase of not-treated (NT) pulp–peel mixtures and ultrasonically treated (T) mixtures with the selected treatment condition (T100 45). PU80 – 80% pulp, 20% peel, PU50 – 50% pulp, 50% peel, PU20 – 20% pulp, 80% peel. Different letters indicate significant differences between samples ( $p < 0.05$ ); lowercase: differences in PLIR, capitalized: differences in AAIR.



untreated control at all adsorption peaks. Alterations were observed at  $3292\text{ cm}^{-1}$  in PU50 and PU20 which indicated the destruction of intramolecular bondings of OH-groups of the cellulose and hemicellulose fraction by US in the mixtures with a higher proportion of orange peel.<sup>27</sup> Bands at  $2922\text{ cm}^{-1}$  and  $2852\text{ cm}^{-1}$  are associated with alkyl chains of polysaccharides<sup>73</sup> and hydroxyl groups of cellulose<sup>74</sup> whereas vibration at  $1734\text{ cm}^{-1}$  could be assigned to acetyl and uronic ester groups of hemicellulose<sup>75</sup> which was particularly prominent in PU80, thus orange pulp. Mixture PU20 showed lower reduction of the intensities of these three bands than PU80 and PU50 which suggested higher resistance of the corresponding structural areas of orange peel. Untreated pulp–peel mixtures highly differed in the intensities of the  $1606\text{ cm}^{-1}$  band while PU20 exhibited the sharpest peak. This band is derived from aromatic benzene groups of lignin,<sup>76</sup> thus a higher intensity would reflect a higher lignin content in orange peel. The reduction of this band after treatments, particularly in PU20, implied the degradation of lignin to phenolic components, seen by the enhanced TPC of this mixture. In addition, bands from  $1440$  to  $1200\text{ cm}^{-1}$  were related to  $-\text{CH}$  and  $-\text{CH}_2$  bending vibrations of polysaccharides.<sup>74,77</sup> Variations might indicate the release of cellulosic and hemicellulosic DF components by US which have changed the accessibility of hydrophobic functional groups. Intensities are most weakened in PU50 suggesting a potential correlation with the enhanced OHC. The extensive vibration at  $1013\text{ cm}^{-1}$  was due to stretching vibration of carboxyl groups,<sup>78</sup> while the sharper peak of PU80 might indicate higher accessibility of these groups in orange pulp. Together with the elevated intensity of  $1734\text{ cm}^{-1}$ , which was linked with the increased presence of hydrophilic hemicellulosic groups in orange pulp, these groups might have caused higher WHC, CAC and AAIR in PU80. Finally,  $665\text{ cm}^{-1}$  originated from the absorbance of benzene rings from the lignin fraction.<sup>74</sup> When comparing the untreated mixtures, the higher intensity of PU20 confirmed the higher content of lignin associated with the higher TPC.

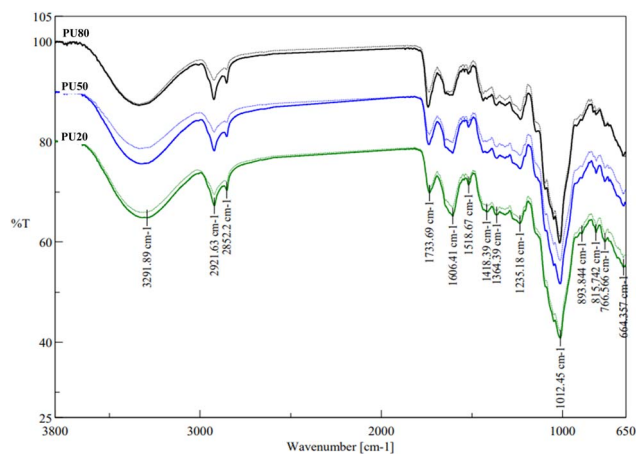


Fig. 5 ATR-FTIR spectra from  $650$  to  $3800\text{ cm}^{-1}$  for untreated and ultrasonically treated (T100 45) orange pulp–peel mixtures. PU80 – 80% pulp, 20% peel (black), PU50 – 50% pulp, 50% peel (blue), PU20 – 20% pulp, 80% peel (green), bold line – untreated, dotted line – treated.

## 4 Conclusion

The application of US treatments showed high potential in improving the structural, water-binding and health-related properties, particularly PLIR and AAIR, of orange by-products. Results could demonstrate that powder mixtures containing different quantities of orange pulp and peel exhibited unique properties and responded differently to the application of US cavitation. Mixtures comprised of a higher content of orange pulp demonstrated higher improvements in techno-functional and health-related properties after US, excluding BAC and TPC. Contrastingly, PU20 containing the highest amount of orange peel showed higher particle size and resistance to US energy but higher TPC after treatments which led to increased BAC. Since the increase in solubility was minimal, changes of techno-functional and health-promoting properties in the ultrasonicated mixtures are primarily related to the opened IDF structure and higher availability of certain functional groups rather than a shift in IDF/SDF ratios.

In conclusion, the health effect of orange by-products and the effectiveness of US depend on the selected amounts of the different fractions, *i.e.* pulp and peel. Both treated by-products offer distinct advantages in their application and their proportion within mixtures could be selected according to the desired objective of their incorporation.

## Data availability

The data that support the findings of this study are openly available in CORA – Repositori de Dades de Recerca at <https://doi.org/10.34810/data1516>.

## Author contributions

Alina Manthei: conceptualization; methodology; investigation; writing – original draft, review and editing. Pedro Elez-Martínez: funding acquisition, writing – review and editing. Olga Martín-Belloso: writing – review and editing. Robert Soliva-Fortuny: conceptualization; supervision; writing – review and editing.

## Conflicts of interest

There are no conflicts of interest to declare.

## Acknowledgements

This work has received funding from the European Union's H2020 research and innovation programme under Marie Skłodowska-Curie grant agreement No. 801586. The project RTI2018-095560-B-I00 was funded by MCIN/AEI/10.13039/501100011033/and FEDER ('A way of making Europe') and the project TED2021-131828B-I00 was financed by MCIN/AEI/10.13039/501100011033 and European Union NextGenerationEU/PRTR.



## References

- 1 M. F. Neves, V. G. Trombin, V. N. Marques and L. F. Martinez, Global orange juice market: a 16-year summary and opportunities for creating value, *Trop. Plant Pathol.*, 2020, **45**(3), 166–174.
- 2 M. V. Vilariño, C. Franco and C. Quarrington, Food loss and waste reduction as an integral part of a circular economy, *Front. Environ. Sci.*, 2017, **5**, 21.
- 3 F. T. Macagnan, L. R. D. Santos, B. S. Roberto, F. A. De Moura, M. Bizzani and L. P. Da Silva, Biological properties of apple pomace, orange bagasse and passion fruit peel as alternative sources of dietary fibre, *Bioact. Carbohydr. Diet. Fibre*, 2015, **6**(1), 1–6.
- 4 N. O'Shea, E. K. Arendt and E. Gallagher, Dietary fibre and phytochemical characteristics of fruit and vegetable by-products and their recent applications as novel ingredients in food products, *Innovative Food Sci. Emerging Technol.*, 2012, **16**, 1–10.
- 5 J. M. Jones, CODEX-aligned dietary fiber definitions help to bridge the “fiber gap.”, *Nutr. J.*, 2014, **13**(1), 34.
- 6 C. W. C. Kendall, A. Esfahani and D. J. A. Jenkins, The link between dietary fibre and human health, *Food Hydrocolloids*, 2010, **24**(1), 42–48.
- 7 F. T. Macagnan, F. A. De Moura, L. R. Dos Santos, M. Bizzani and L. P. Da Silva, Caracterização nutricional e resposta sensorial de pães de mel com alto teor de fibra alimentar elaborados com farinhas de subprodutos do processamento de frutas, *Bol. do Cent. Pesqui. Process. Aliment.*, 2014, **32**(2), 201–210.
- 8 C. F. Chau and Y. L. Huang, Comparison of the chemical composition and physicochemical properties of different fibers prepared from the peel of citrus sinensis L. Cv. Liucheng, *J. Agric. Food Chem.*, 2003, **51**(9), 2615–2618.
- 9 R. Casquete, S. M. Castro, A. Martín, S. Ruiz-Moyano, J. A. Saraiva, M. G. Córdoba, *et al.*, Evaluation of the effect of high pressure on total phenolic content, antioxidant and antimicrobial activity of citrus peels, *Innovative Food Sci. Emerging Technol.*, 2015, **31**, 37–44.
- 10 A. Iqbal, P. Schulz and S. S. H. Rizvi, Valorization of bioactive compounds in fruit pomace from agro-fruit industries: Present Insights and future challenges, *Food Biosci.*, 2021, **44**, 101384.
- 11 A. P. Espírito-Santo, A. Lagazzo, A. L. O. P. Sousa, P. Perego, A. Converti and M. N. Oliveira, Rheology, spontaneous whey separation, microstructure and sensorial characteristics of probiotic yoghurts enriched with passion fruit fiber, *Food Res. Int.*, 2013, **50**(1), 224–231.
- 12 N. Grigelmo-Miguel and O. Martín-Belloso, Comparison of Dietary Fibre from By-products of Processing Fruits and Greens and from Cereals, *LWT-Food Sci. Technol.*, 1999, **32**(8), 503–508.
- 13 I. F. Strati, E. Gogou and V. Oreopoulou, Enzyme and high pressure assisted extraction of carotenoids from tomato waste, *Food Bioprod. Process.*, 2015, **94**, 668–674.
- 14 J. Pérez-Jiménez and F. Saura-Calixto, Fruit peels as sources of non-extractable polyphenols or macromolecular antioxidants: Analysis and nutritional implications, *Food Res. Int.*, 2018, **111**, 148–152.
- 15 A. D. Blackwood, J. Salter, P. W. Dettmar and M. F. Chaplin, Dietary fibre, physicochemical properties and their relationship to health, *J. Roy. Soc. Promot. Health*, 2000, **120**(4), 242–247.
- 16 D. Mudgil, The Interaction Between Insoluble and Soluble Fiber, in *Dietary Fiber for the Prevention of Cardiovascular Disease*, 2017, pp. 35–59.
- 17 F. Zhang, W. Yi, J. Cao, K. He, Y. Liu and X. Bai, Microstructure characteristics of tea seed dietary fibre and its effect on cholesterol, glucose and nitrite ion adsorption capacities in vitro: a comparison study among different modifications, *Int. J. Food Sci. Technol.*, 2020, **55**(4), 1781–1791.
- 18 L. Huang, X. Ding, Y. Zhao, Y. Li and H. Ma, Modification of insoluble dietary fiber from garlic straw with ultrasonic treatment, *J. Food Process. Preserv.*, 2018, **42**(1), e13399.
- 19 T. V. Fonteles, A. K. F. Leite, A. R. A. da Silva, F. A. N. Fernandes and S. Rodrigues, Sonication Effect on Bioactive Compounds of Cashew Apple Bagasse, *Food Bioprocess Technol.*, 2017, **10**(10), 1854–1864.
- 20 M. Ashokkumar, D. Sunartio, S. Kentish, R. Mawson, L. Simons, K. Vilku, *et al.*, Modification of food ingredients by ultrasound to improve functionality: A preliminary study on a model system, *Innovative Food Sci. Emerging Technol.*, 2008, **9**(2), 155–160.
- 21 C. Gong and D. P. Hart, Ultrasound induced cavitation and sonochemical yields, *J. Acoust. Soc. Am.*, 1998, **104**, 1–16.
- 22 S. A. Moreira, E. M. C. Alexandre, M. Pintado and J. A. Saraiva, Effect of emergent non-thermal extraction technologies on bioactive individual compounds profile from different plant materials, *Food Res. Int.*, 2019, **11**, 177–190.
- 23 K. Kumar, S. Srivastav and V. S. Sharanagat, Ultrasound assisted extraction (UAE) of bioactive compounds from fruit and vegetable processing by-products: A review, *Ultrason. Sonochem.*, 2021, **70**, 105325.
- 24 N. A. Sagar, S. Pareek, S. Sharma, E. M. Yahia and M. G. Lobo, Fruit and Vegetable Waste: Bioactive Compounds, Their Extraction, and Possible Utilization, *Compr. Rev. Food Sci. Food Saf.*, 2018, **17**(3), 512–531.
- 25 F. Sarpong, X. Yu, C. Zhou, Y. Hongpeng, B. B. Uzoejinwa, J. Bai, *et al.*, Influence of anti-browning agent pretreatment on drying kinetics, enzymes inactivation and other qualities of dried banana (*Musa ssp.*) under relative humidity-convective air dryer, *J. Food Meas. Char.*, 2018, **12**(2), 1229–1241.
- 26 J. A. Robertson, F. D. De Monredon, P. Dysseler, F. Guillon, R. Amadò and J. F. Thibault, Hydration properties of dietary fibre and resistant starch: A European collaborative study, *LWT-Food Sci. Technol.*, 2000, **33**(2), 72–79.
- 27 M. M. Ma and T. H. Mu, Effects of extraction methods and particle size distribution on the structural,



- physicochemical, and functional properties of dietary fiber from deoiled cumin, *Food Chem.*, 2016, **194**, 237–246.
- 28 H. Xu, Q. Jiao, F. Yuan and Y. Gao, In vitro binding capacities and physicochemical properties of soluble fiber prepared by microfluidization pretreatment and cellulase hydrolysis of peach pomace, *LWT–Food Sci. Technol.*, 2015, **63**(1), 677–684.
  - 29 J. Chu, H. Zhao, Z. Lu, F. Lu, X. Bie and C. Zhang, Improved physicochemical and functional properties of dietary fiber from millet bran fermented by *Bacillus natto*, *Food Chem.*, 2019, **294**(1), 79–86.
  - 30 L. E. Garcia-Amezquita, V. Tejada-Ortigoza, O. H. Campanella and J. Welti-Chanes, Influence of Drying Method on the Composition, Physicochemical Properties, and Prebiotic Potential of Dietary Fibre Concentrates from Fruit Peels, *J. Food Qual.*, 2018, **2018**, 9105237.
  - 31 K. Yang, Z. Yang, W. Wu, H. Gao, C. Zhou, P. Sun, *et al.*, Physicochemical properties improvement and structural changes of bamboo shoots (*Phyllostachys praecox* f. *Prevernalis*) dietary fiber modified by subcritical water and high pressure homogenization: a comparative study, *J. Food Sci. Technol.*, 2020, **57**(10), 3659–3666.
  - 32 V. Benitez, M. Rebollo-hernanz, S. Hernanz and S. Chantres, Coffee parchment as a new dietary fiber ingredient: Functional and physiological characterization, *Food Res. Int.*, 2019, **122**, 105–113.
  - 33 V. S. Schneider, J. M. Bark, S. M. B. Winnischofer, E. F. Dos Santos, M. Iacomini and L. M. C. Cordeiro, Dietary fibres from guavira pomace, a co-product from fruit pulp industry: Characterization and cellular antioxidant activity, *Food Res. Int.*, 2020, **132**, 109065.
  - 34 R. Re, N. Pellegrini, A. Proteggente, A. Pannala, M. Yang and C. Rice-Evans, Antioxidant activity applying an improved ABTS radical cation decolorization assay, *Free Radic. Biol. Med.*, 1999, **26**, 1231–1237.
  - 35 G. López, G. Ros, F. Rincón, M. J. Periago, M. C. Martínez and J. Ortuño, Relationship between Physical and Hydration Properties of Soluble and Insoluble Fiber of Artichoke, *J. Agric. Food Chem.*, 1996, **44**, 2773–2778.
  - 36 M. F. Chaplin, Fibre and water binding, *Proc. Nutr. Soc.*, 2003, **62**(1), 223–227.
  - 37 Y. L. Huang and Y. S. Ma, The effect of extrusion processing on the physicochemical properties of extruded orange pomace, *Food Chem.*, 2016, **192**, 363–369.
  - 38 G. Yu, J. Bei, J. Zhao, Q. Li and C. Cheng, Modification of carrot (*Daucus carota* Linn. var. *Sativa* Hoffm.) pomace insoluble dietary fiber with complex enzyme method, ultrafine comminution, and high hydrostatic pressure, *Food Chem.*, 2018, **257**, 333–340.
  - 39 C. Zacherl, P. Eisner and K. H. Engel, In vitro model to correlate viscosity and bile acid-binding capacity of digested water-soluble and insoluble dietary fibres, *Food Chem.*, 2011, **126**(2), 423–428.
  - 40 Y. Hamauzu and J. Suwannachot, Non-extractable polyphenols and in vitro bile acid-binding capacity of dried persimmon (*Diospyros kaki*) fruit, *Food Chem.*, 2019, **293**, 127–133.
  - 41 N. Zhang, C. Huang and S. Ou, In vitro binding capacities of three dietary fibers and their mixture for four toxic elements, cholesterol, and bile acid, *J. Hazard. Mater.*, 2011, **186**, 236–239.
  - 42 I. Navarro-González, V. García-Valverde, J. García-Alonso and M. J. Periago, Chemical profile, functional and antioxidant properties of tomato peel fiber, *Food Res. Int.*, 2011, **44**, 1528–1535.
  - 43 F. Guillon and M. Champ, Structural and physical properties of dietary fibres, and consequences of processing on human physiology, *Food Res. Int.*, 2000, **33**(3–4), 233–245.
  - 44 Y. L. Huang, Y. S. Ma, Y. H. Tsai and S. K. C. Chang, In vitro hypoglycemic, cholesterol-lowering and fermentation capacities of fiber-rich orange pomace as affected by extrusion, *Int. J. Biol. Macromol.*, 2019, **124**, 796–801.
  - 45 F. Figuerola, M. L. Hurtado, A. M. Estévez, I. Chiffelle and F. Asenjo, Fibre concentrates from apple pomace and citrus peel as potential fibre sources for food enrichment, *Food Chem.*, 2005, **91**(3), 395–401.
  - 46 H. Bengtsson, C. Hall and E. Tornberg, Effect of physicochemical properties on the sensory perception of the texture of homogenized fruit and vegetable fiber suspensions, *J. Texture Stud.*, 2011, **42**(4), 291–299.
  - 47 R. C. Rivas-Cantu, K. D. Jones and P. L. Mills, A citrus waste-based biorefinery as a source of renewable energy: Technical advances and analysis of engineering challenges, *Waste Manage. Res.*, 2013, 413–420.
  - 48 L. E. Garcia-Amezquita, V. Tejada-Ortigoza, E. Pérez-Carrillo, S. O. Serna-Saldivar, O. H. Campanella and J. Welti-Chanes, Functional and compositional changes of orange peel fiber thermally-treated in a twin extruder, *LWT*, 2019, **111**, 673–681.
  - 49 V. Tejada-Ortigoza, L. E. Garcia-Amezquita, S. O. Serna-Saldivar, O. Martin-Belloso and J. Welti-Chanes, High Hydrostatic Pressure and Mild Heat Treatments for the Modification of Orange Peel Dietary Fiber: Effects on Hygroscopic Properties and Functionality, *Food Bioprocess Technol.*, 2018, **11**(1), 110–121.
  - 50 Y. L. Huang and Y. S. Ma, The effect of extrusion processing on the physicochemical properties of extruded orange pomace, *Food Chem.*, 2016, **192**, 363–369.
  - 51 V. Athanasiadis, T. Chatzimitakos, K. Kotsou, D. Palaogiannis, E. Bozinou and S. I. Lalas, Optimization of the Extraction Parameters for the Isolation of Bioactive Compounds from Orange Peel Waste, *Sustainability*, 2022, **14**(21), 13926.
  - 52 M. Abbas, F. Saeed, F. M. Anjum, M. Afzaal, T. Tufail, M. S. Bashir, *et al.*, Natural polyphenols: An overview, *Int. J. Food Prop.*, 2017, **20**(8), 1689–1699.
  - 53 Z. Jiang, S. Mu, C. Ma, Y. Liu, Y. Ma, M. Zhang, *et al.*, Consequences of ball milling combined with high-pressure homogenization on structure, physicochemical and rheological properties of citrus fiber, *Food Hydrocolloids*, 2022, **127**, 107515.
  - 54 U. C. Lohani, K. Muthukumarappan and G. H. Meletharayil, Application of hydrodynamic cavitation to improve





- antioxidant activity in sorghum flour and apple pomace, *Food Bioprod. Process.*, 2016, **100**, 335–343.
- 55 R. A. L. Jutkus, N. Li, L. S. Taylor and L. J. Mauer, Effect of temperature and initial moisture content on the chemical stability and color change of various forms of Vitamin C, *Int. J. Food Prop.*, 2015, **18**(4), 862–879.
  - 56 D. C. Murador, A. R. C. Braga, P. L. G. Martins, A. Z. Mercadante and V. V. de Rosso, Ionic liquid associated with ultrasonic-assisted extraction: A new approach to obtain carotenoids from orange peel, *Food Res. Int.*, 2019, **126**, 108653.
  - 57 L. Galván D'Alessandro, K. Dimitrov, P. Vauchel and I. Nikov, Kinetics of ultrasound assisted extraction of anthocyanins from Aronia melanocarpa (black chokeberry) wastes, *Chem. Eng. Res. Des.*, 2014, **92**(10), 1818–1826.
  - 58 Ö. Aybastier, E. Işık, S. Şahin and C. Demir, Optimization of ultrasonic-assisted extraction of antioxidant compounds from blackberry leaves using response surface methodology, *Ind. Crops Prod.*, 2013, **44**, 558–565.
  - 59 S. Naumann, U. Schweiggert-Weisz and P. Eisner, Characterisation of the molecular interactions between primary bile acids and fractionated lupin cotyledons (*Lupinus angustifolius* L.), *Food Chem.*, 2020, **323**, 126780.
  - 60 G. Fontana, The Orange Peel: An Outstanding Source of Chemical Resources, in *Citrus – Research, Development and Biotechnology*, 2021.
  - 61 E. Capuano, The behavior of dietary fiber in the gastrointestinal tract determines its physiological effect, *Crit. Rev. Food Sci. Nutr.*, 2017, **57**(16), 3543–3564.
  - 62 C. M. Huang and N. H. Dural, Adsorption of bile acids on cereal type food fibers, *J. Food Process. Eng.*, 1995, **18**, 243–266.
  - 63 G. Rodríguez-Gutiérrez, F. Rubio-Senent, A. Lama-Muñoz, A. García and J. Fernández-Bolaños, Properties of lignin, cellulose, and hemicelluloses isolated from olive cake and olive stones: Binding of water, oil, bile acids, and glucose, *J. Agric. Food Chem.*, 2014, **62**(36), 8973–8981.
  - 64 D. Lin, X. Long, Y. Huang, Y. Yang, Z. Wu, H. Chen, *et al.*, Effects of microbial fermentation and microwave treatment on the composition, structural characteristics, and functional properties of modified okara dietary fiber, *LWT–Food Sci. Technol.*, 2020, **123**, 109059.
  - 65 L. Yan, T. Li, C. Liu and L. Zheng, Effects of high hydrostatic pressure and superfine grinding treatment on physicochemical/functional properties of pear pomace and chemical composition of its soluble dietary fibre, *LWT–Food Sci. Technol.*, 2019, **107**, 171–177.
  - 66 A. Tamargo, D. Martín, J. Navarro del Hierro, M. V. Moreno-Arribas and L. A. Muñoz, Intake of soluble fibre from chia seed reduces bioaccessibility of lipids, cholesterol and glucose in the dynamic gastrointestinal model simgi®, *Food Res. Int.*, 2020, **137**, 109364.
  - 67 A. Kumar and S. Chauhan, Pancreatic lipase inhibitors: The road voyaged and successes, *Life Sci.*, 2021, **271**, 119115.
  - 68 R. Huang, Y. Zhang, S. Shen, Z. Zhi, H. Cheng, S. Chen, *et al.*, Antioxidant and pancreatic lipase inhibitory effects of flavonoids from different citrus peel extracts: An in vitro study, *Food Chem.*, 2020, **326**, 126785.
  - 69 H. Zhai, P. Gunness and M. J. Gidley, Depletion and bridging flocculation of oil droplets in the presence of  $\beta$ -glucan, arabinoxylan and pectin polymers: Effects on lipolysis, *Carbohydr. Polym.*, 2021, **255**, 117491.
  - 70 M. Espinal-Ruiz, F. Parada-Alfonso, L. P. Restrepo-Sánchez, C. E. Narváez-Cuenca and D. J. McClements, Impact of dietary fibers [methyl cellulose, chitosan, and pectin] on digestion of lipids under simulated gastrointestinal conditions, *Food Funct.*, 2014, **5**(12), 3083–3095.
  - 71 S. Dhital, M. J. Gidley and F. J. Warren, Inhibition of  $\alpha$ -amylase activity by cellulose: Kinetic analysis and nutritional implications, *Carbohydr. Polym.*, 2015, **123**, 305–312.
  - 72 Y. Bai, S. Atluri, Z. Zhang, M. J. Gidley, E. Li and R. G. Gilbert, Structural reasons for inhibitory effects of pectin on  $\alpha$ -amylase enzyme activity and in-vitro digestibility of starch, *Food Hydrocolloids*, 2021, **114**, 106581.
  - 73 L. H. Velazquez-Jimenez, A. Pavlick and J. R. Rangel-Mendez, Chemical characterization of raw and treated agave bagasse and its potential as adsorbent of metal cations from water, *Ind. Crops Prod.*, 2013, **43**(1), 200–206.
  - 74 L. wen Song, J. ru Qi, L. J. song and Y. X. quan, Enzymatic and enzyme-physical modification of citrus fiber by xylanase and planetary ball milling treatment, *Food Hydrocolloids*, 2021, **121**, 107015.
  - 75 B. Yang, Q. Wu, X. Song, Q. Yang and J. Kan, Physicochemical properties and bioactive function of Japanese grape (*Hovenia dulcis*) pomace insoluble dietary fibre modified by ball milling and complex enzyme treatment, *Int. J. Food Sci. Technol.*, 2019, **54**(7), 2363–2373.
  - 76 D. Wang, X. Liu, K. Wang, L. Zhao, Y. Wang, X. Zhang, *et al.*, Impact of non-thermal modifications on the physicochemical properties and functionality of litchi pomace dietary fibre, *LWT*, 2023, **182**, 114878.
  - 77 H. J. Yi, J. S. Liao, J. R. Qi, W. X. Jiang and X. Q. Yang, Structural and physicochemical properties of pectin-rich dietary fiber prepared from citrus peel, *Food Hydrocolloids*, 2021, **110**, 106140.
  - 78 Y. Zheng and Y. Li, Physicochemical and functional properties of coconut (*Cocos nucifera* L) cake dietary fibres: Effects of cellulase hydrolysis, acid treatment and particle size distribution, *Food Chem.*, 2018, **257**, 135–142.

